HETEROCYCLES, Vol. 101, No. 2, 2020, pp. 536 - 547. © 2020 The Japan Institute of Heterocyclic Chemistry
Received, 30th June, 2019, Accepted, 26th August, 2019, Published online, 7th October, 2019
DOI: 10.3987/COM-19-S(F)44

SYNTHESIS AND OPTICAL PROPERTIES OF L-SHAPED DINAPHTHOFLUORESCEINS WITH TWO PERIPHERAL HYDROXY GROUPS

Hikari Yamashita,[a] Chihiro Minari,[a] Eriko Azuma,[a] Kouji Kuramochi,[b] Ayumi Imayoshi,[a] and Kazunori Tsubaki[a]*

[a)] Graduate School of Life and Environmental Sciences, Kyoto Prefectural University, Shimogamo, Sakyo-ku, Kyoto 606-8522, Japan. [b)] Department of Applied Biological Science, Faculty of Science and Technology, Tokyo University of Science, 2641 Yamazaki, Noda, Chiba 278-8510, Japan. E-mail:tsubaki@kpu.ac.jp

This paper is dedicated to Professor Kaoru Fuji in celebration of his 80th birthday.

Abstract – The four compounds **6** and **8**–**10** having the same L-shaped dinaphthofluorescein skeleton were constructed. The only structural differences among these four compounds were the positions of the two peripheral hydroxy groups. Their dianion forms are a resonance system, thus **6** and **8**–**10** were expected to exhibit similar optical properties such as the maximum absorption wavelength, molar absorptivity, maximum emission wavelength and fluorescence quantum yield. However, **6** and **8**–**10** showed quite different optical properties. For example, the maximum absorption wavelengths of **6**, **8**, **9** and **10** in aqueous pH 11 solution were 650 nm, 733 nm, 558 nm and 746 nm, respectively. Thus, the positions of the two peripheral hydroxy groups on the same skeleton significantly affected the optical properties.

INTRODUCTION

Fluorescent dyes are widely used in molecular biology, especially for the detection of localized target molecules in cells and/or tissue.[1] Fluorescent dyes such as fluorescein (**1**) have absorption and emission wavelengths in the visible region. It is problematic for use in bio-imaging where they overlap with the autofluorescence from the living body. Fluorescent dyes that can be excited and emit at longer wavelengths are therefore desirable, to avoid any overlap with the autofluorescence.[2] In pursuit of useful

fluorescent dyes, we previously synthesized dinaphthofluoresceins **2**–**7**, in which additional benzene rings were added to the left and right of the fluorescein (**1**) skeleton, and we evaluated their optical properties (Figure 1).[3]

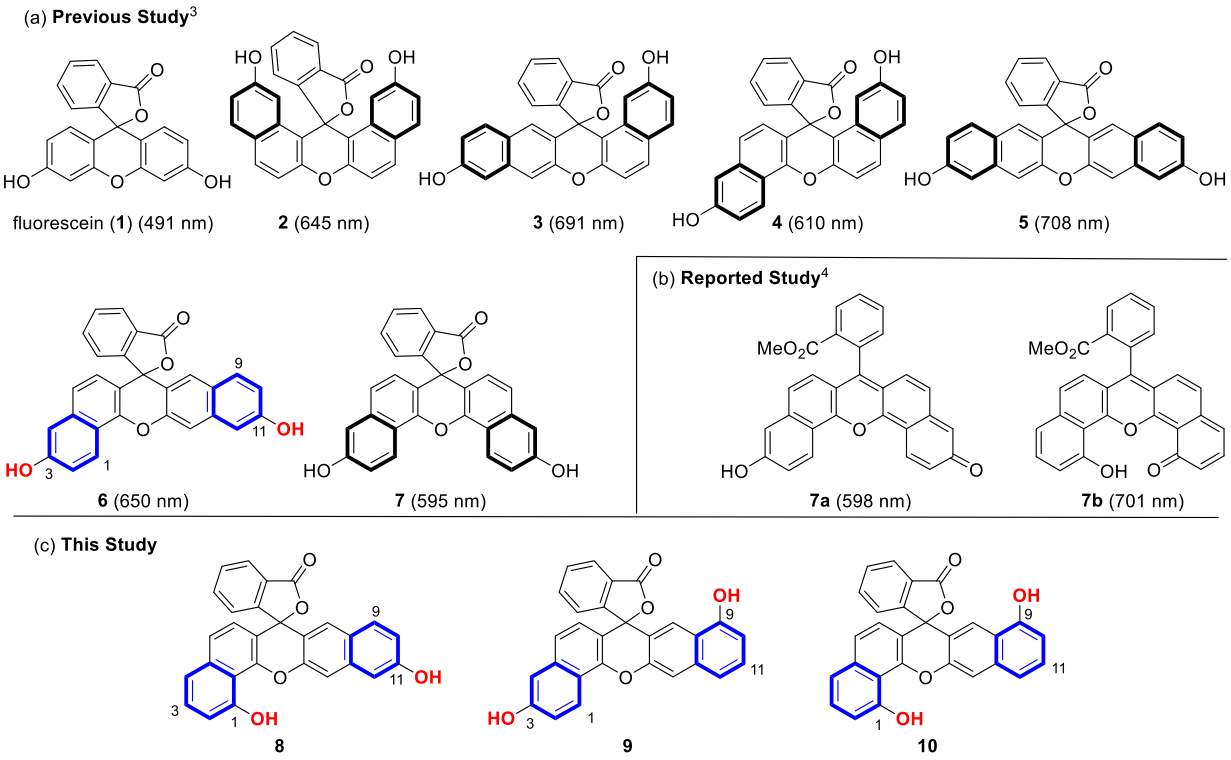

(a) Previously synthesized dinaphthofluoresceins **2**–**7**. Values in parentheses indicate the maximum absorption wavelength at pH 11. (b) Related compounds **7a** and **7b** reported by Strongin *et al.*[4] (c) L-Shaped dinaphthofluoresceins **8**–**10** reported in the current study.

Figure 1. Structures of fluorescein and related compounds

That study afforded the following findings about the relationship between the directions of the additionally condensed benzene rings and the optical properties of the overall dinaphthofluorescein. First, compound **5** in which the aromatic rings were linearly aligned showed the largest red shifts of absorption and emission wavelengths among the six dinaphthofluoresceins. Second, known compound **7** which retained a bell-shape arrangement of aromatic rings showed the highest quantum yield and smallest red shifts of absorption and emission wavelengths.[5] Third, L-shaped dinaphthofluorescein **6**, in which one additional benzene ring was in the lateral direction and the other was in the downward direction, showed broader absorption and emission wavelengths and the quantum yield was also improved compared with that of the linear compound **5**.

The present study focuses on the L-shaped dinaphthofluorescein **6** and the related compounds **8**–**10**, in which the two hydroxy groups of compound **6** are shifted to other appropriate resonance positions. We investigated the effects of the position of the two hydroxy groups on the absorption/emission wavelengths as well as the fluorescent quantum yields (Figure 1c). Strongin *et al*. reported compounds **7a** and **7b**, with the hydroxy groups in compound **7b** directed towards the inside.[4,6] They reported a large red shift of about 100 nm in the absorption wavelength of compound **7b** compared with that of compound **7a**. In the present study, we also compare the optical properties of compounds **7a** and **7b** and with those of compounds **6** and **8**–**10**.

RESULTS AND DISCUSSION

Scheme 1 shows the synthetic routes for the L-shaped dinaphthofluoresceins **8**–**10** possessing two hydroxy groups at various positions. The framework of the dinaphthofluorescein can be constructed through the Friedel-Crafts reaction of the corresponding 2-aroylbenzoic acid and appropriate dihydroxynaphthalene under acidic conditions. That is, the target compound **8** was synthesized from aroylbenzoic acid **11**[3] and 1,8-dihydroxynaphthalene (**12**) in a mixed solvent of methanesulfonic acid and toluene in 52% yield. The aroylbenzoic acid **15**, which is a common key intermediate for compounds **9** and **10**, was also constructed. Compound **13**[7] was treated with *n*-butyllithium and trapped with iodine to give a mixture of the desired intermediate **A** and the recovered starting material **13** in ca. 1:1 ratio. The mixture was used for the next step without further purification.

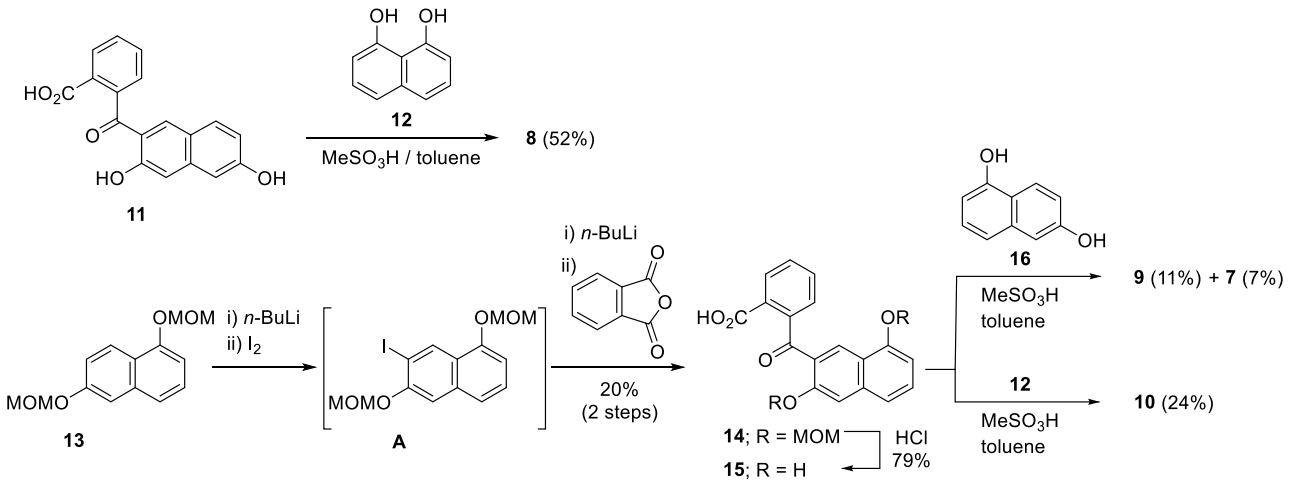

Scheme 1. Synthesis of dinaphthofluoresceins **8**–**10**

The crude **A** was lithiated with *n*-butyllithium and then reacted with phthalic anhydride to afford aroylbenzoic acid **14** in 20% overall yield for the two steps. Two MOM groups in compound **14** were removed by hydrochloric acid to afford the common intermediate **15** in 79% yield. The aroylbenzoic acid

15 was coupled with 1,6-dihydroxynaphthalene (**16**) to afford compounds **9** and **7** in yields of 11% and 7%, respectively. The isomer **7** should be generated from the retro Friedel-Crafts reaction of compound **15** and then the double normal phase Friedel-Crafts reaction of the obtained phthalic anhydride and 1,6-dihydroxynaphthalene (**16**). Finally, the reaction of compound **15** with 1,8-dihydroxynaphthalene (**12**) produced the target compound **10** in 24% yield. With a series of L-shaped dinaphthofluoresceins **6** and **8**–**10** in hand, we then evaluated their optical properties.

Compounds **6** and **8**–**10** are π-expanded fluorescein derivatives, thus they should inherit similar properties to those of the parent fluorescein (**1**). We first examined their color responses under various aqueous pH solutions (Figure 2). Due to the low solubility of these compounds in aqueous solution, precipitation was observed mainly under acidic conditions, and no significant coloration (except for under extreme acidity; *i.e.* aqueous $MeSO_3H$) was observed. Under basic conditions the two phenolic hydroxy groups dissociated, and clear coloration was observed in homogeneous solution. The coloration of solutions of compounds **6** and **8**–**10** is discussed below.

Dinaphthofluorescein **6** developed a dark purple color under strongly acidic conditions (pH −1~1) and precipitates were observed at pH 3~7. In the basic region, compound **6** showed a pale blue color at pH 8 that gradually became deep blue as the pH increased. Compound **6** then became slightly pale at pH 13 and abruptly turned a red-brown color at pH 14. In the absorption spectra, under highly acidic conditions, compound **6** showed a broad absorption at around 450–700 nm and λ_{max} were observed at 490 nm and 581 nm. In the basic region, compound **6** showed a λ_{max} at 650 nm. At pH 14, the λ_{max} of compound **6** was blue shifted to 476 nm. Compound **8** was bright blue-green at pH −1 with λ_{max} observed at 448 nm and 639 nm. In the basic region, compound **8** was green and the λ_{max} was 733 nm. Compared with compound **6**, changing the position of the hydroxy group from the outside to inside caused a large red shift of about 83 nm in the absorption spectra. At pH 14, the color also abruptly changed to bright red. Dinaphthofluorescein **9** turned pale purple at pH 9, became deep purple at pH 10~12, slightly reddish brown at pH 13 and finally orange at pH 14. While a shoulder peak probably existed at around 720 nm, the λ_{max} of compound **9** was at around 558 nm under basic conditions, and the λ_{max} (558 nm) was largely blue shifted compared with the other compounds (650 nm and 733 nm for compounds **6** and **8**, respectively). The intensity of the coloration of compound **9** was smaller than that of compounds **6** and **8**. Dinaphthofluorescein **10** had a λ_{max} at 746 nm in the basic region. However, compound **10** showed weak and vague coloration compared with the other compounds. Judging from its coloration, compound **10** was considered to be unsuitable as a color indicator.

The color development of these dinaphthofluoresceins in response to pH can be explained as follows (compound **8** is used as a representative compound).

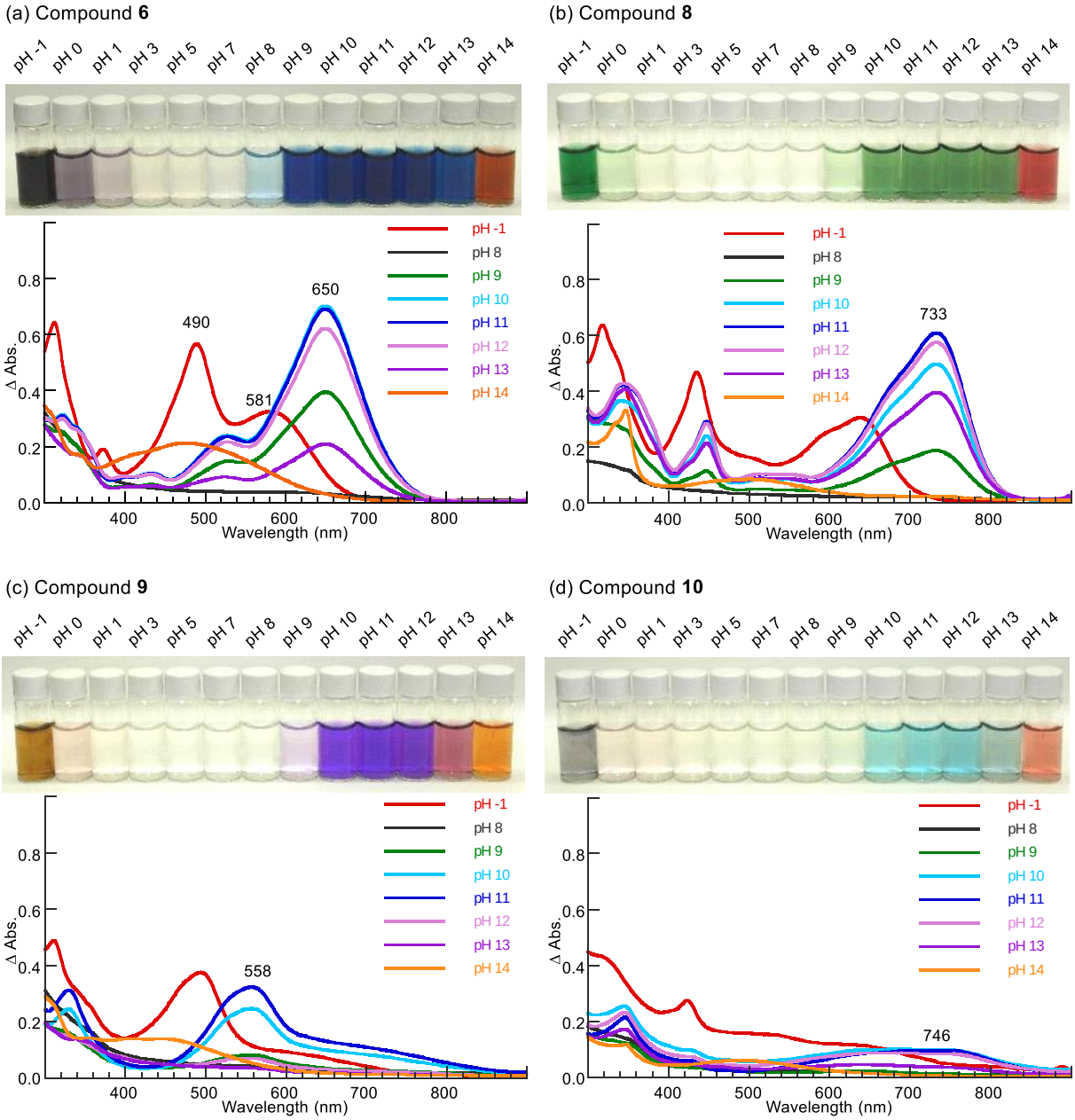

Conditions; photo; [compound] = 1.0×10^{-4} M, UV-vis absorption spectra; [compound] = 2.0×10^{-5} M, $MeSO_3H$ aq. (pH –1), HCl-KCl buffer (pH 1), citrate-phosphate buffer (pH 3, 5, 7), tris-HCl buffer (pH 8, 9), glycine-NaOH buffer (pH 10, 11, 12, 13, 14).

Figure 2. Coloration and UV-vis absorption spectra of the dinaphthofluoresceins **6** and **8**–**10** in various pH solutions

Under extreme acidic conditions, after protonation on the lactone carbonyl group, cleavage of the lactone ring takes place by participation of the phenolic hydroxy group to afford colored monocationic $\mathbf{8}^{+}$ that has an expanded π system over the left and right naphthalene rings. In the basic region, protons of the two phenolic hydroxy groups are absorbed by hydroxide ions to generate the colored dianionic species $\mathbf{8}^{2-}$ via monoanionic $\mathbf{8}^{-}$. Under strongly basic conditions, the hydroxide ion attacks the central trityl position, and

the conjugated system of **8** is cleaved to form trianion $\mathbf{8}^{3-}$, which absorbs at a shorter wavelength (Figure 3). The following points are worth mentioning. At the pictures in Figure 2, compounds **6** and **9** are colored from pH 8 and pH 9, respectively. In contrast, compounds **8** and **10** have changed color from pH 10. This indicates that inward hydroxy group at the 1 position of compounds **8** and **10** forms an intramolecular hydrogen bond with the oxygen of the pyran ring, and therefore the colored dianion species of compounds **8** and **10** are less likely to form.

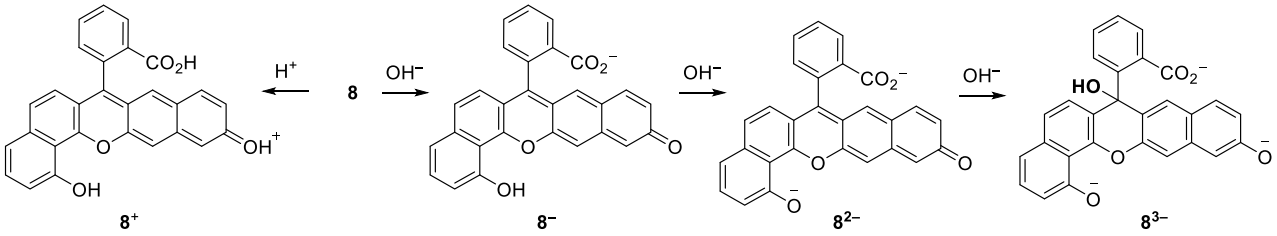

Figure 3. Protonation and deprotonation sequence of compound **8**

Compounds **8** and **10** have hydroxy groups at the 1 position, and showed absorptions at much longer wavelengths (>700 nm) than compounds **6** and **9**. The reasons for this are discussed based on density functional theory (DFT) calculations.[8] Figure 4 shows the highest occupied molecular orbitals (HOMOs), next-HOMO (for compound **9**) and lowest unoccupied molecular orbitals (LUMOs) of dianion species of compounds **6** and **8**–**10** calculated using DFT at the B3LYP/6-31+G(d,p) level of theory with including solvent effects (water). For compound **9**, as shown in Figure 2c, a weak (prohibited) transition at around 720 nm that corresponds to the HOMO-LUMO transition is observed, but the transition has little contribute to the absorption spectrum, so the next-HOMO is used instead. As shown in Figure 4, compounds **8** and **10** having a hydroxy group at the 1 position have less stable HOMOs compared with compounds **6** and **9** having a hydroxy group at the 3 position. The LUMOs of compounds **6** and **8**–**10** are at almost the same level. As a result, the HOMO-LUMO gaps are smaller for compounds **8** and **10** than those for compounds **6** and **9**. This is considered to be the reason why compounds **8** and **10** exhibited long wavelength absorption. The destabilization in the HOMOs of compounds **8** and **10** was caused by the repulsion between the anion of the hydroxy group at position 1 and the oxygen atom of the pyran ring.

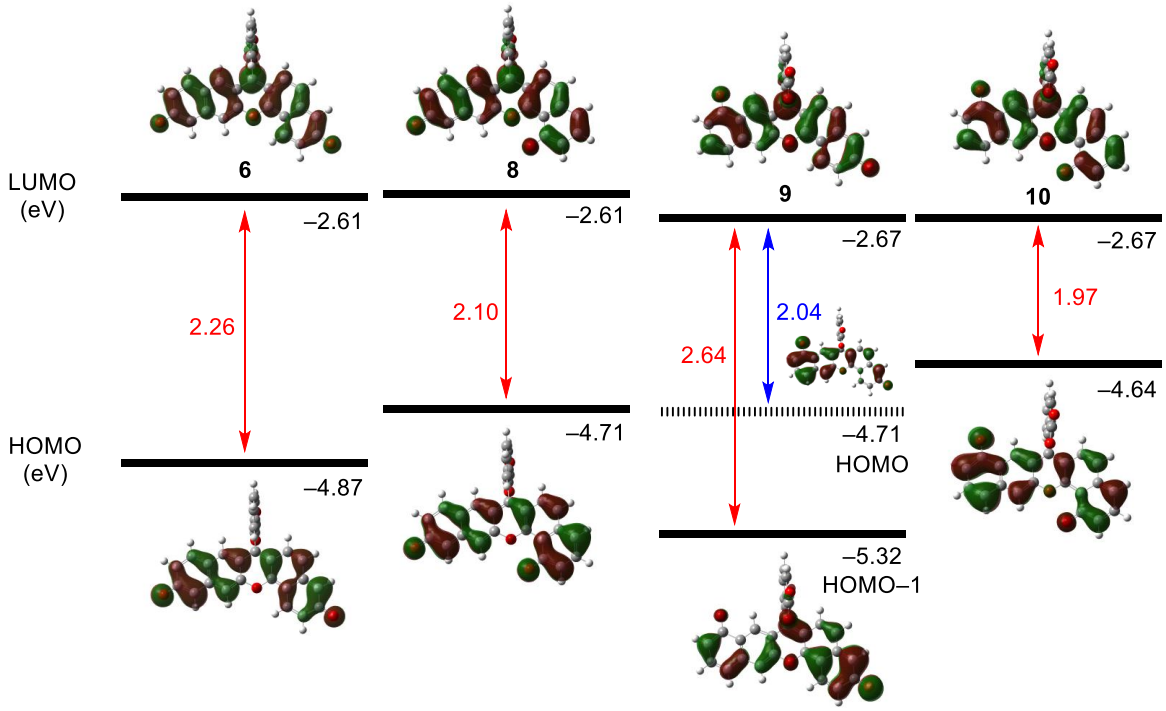

Figure 4. HOMOs, LUMOs, and energy gaps for dianionic **6** and **8–10**, calculated using DFT at the B3LYP/6-31+G(d,p) level of theory with in clouding solvent effects (water)

We previously reported that compound **6** had weak fluorescence properties (i.e. fluorescent quantum yield Φ = 0.4%) in basic solution. Therefore, the fluorescence properties of compounds **8**–**10** were investigated in the current study. Figure 5 shows the normalized fluorescent spectra of **6** and **8**–**10** in aqueous solution at pH 11. Table 1 summarizes the photophysical properties of dinaphthofluoresceins **6** and **8**–**10**, including the maximum absorption wavelength ($\lambda_{abs.\ max}$), maximum molar absorptivity ($\varepsilon_{abs.\ max}$), maximum excitation wavelength ($\lambda_{ex.\ max}$), maximum emission wavelength ($\lambda_{em.\ max}$), fluorescence quantum yield (Φ), Stokes shift measured in buffered solution at pH 11 as well as calculated the maximum absorption wavelength ($\lambda_{abs.\ calcd}$) and oscillator strength (f) using TD-DFT at the B3LYP/6-31+G(d,p) level with including solvent effects (water). Among the dinaphthofluoresceins **6** and **8**–**10**, compound **10** showed no fluorescent under any pH conditions. Compounds **6**, **8**, and **9** all showed fluorescence with fluorescent quantum yields that were generally low. Compound **8** had emission in the near infrared region ($\lambda_{em.\ max}$ = 813 nm).

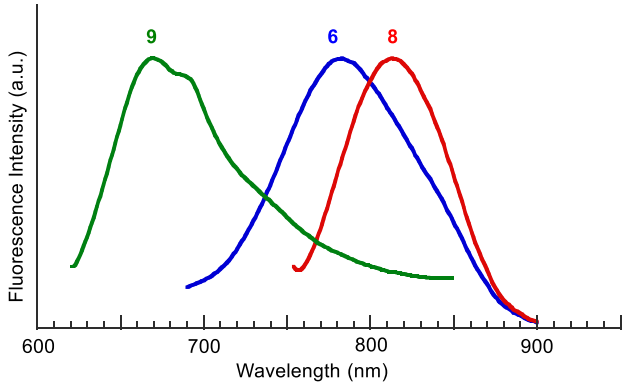

Conditions; glycine-NaOH buffer (pH 11), excitation wavelength; **6** (647 nm), **8** (733 nm), **9** (594 nm).

Figure 5. Fluorescence spectra of compounds **6**, **8** and **9**

Table 1. Observed and calculated photophysical properties of compounds **6** and **8**–**10**

	$\lambda_{abs.max}$ (nm)	ε)$\lambda_{abs.max}$)	$\lambda_{abs.calcd}$ [a] (nm)	f [a,b]	$\lambda_{ex.max}$ (nm)	$\lambda_{em.max}$ (nm)	Φ [c] (%)	S. S[d] (nm)
6	650	34,000	607	0.82	647	780	0.4	133
8	733	30,000	655	0.65	733	813	0.4	80
9	558	16,000	512[e]	0.60	594	670	0.03	76
10	746	4,800	755	0.36	–	–	–	–

Conditions; [**6** and **8**–**10**] = 2.0×10^{-5} M in glycine-NaOH buffer (pH 11). Light pathlength = 1 cm. Temp = 25 ºC. [a] Calculated λabs using TD-DFT at the B3LYP/6-31+G(d,p) level of theory with water as solvent. [b] Oscillator strength. [c] Solution of compound **6** used as a reference standard (Φ = 0.4%). [d] Stokes Shifts. [e] HOMO−1 → LUMO transition.

CONCLUSION

We previously synthesized dinaphthofluoresceins possessing two additional benzene rings incorporated into fluorescein, and clarified the effect of this in the mode of annulation in optical properties. In the current study, four compounds **6** and **8**–**10** having two hydroxy groups at different positions were synthesized using the same L-shaped dinaphthofluorescein skeleton, and their optical properties were examined. Although the resonance structures of the colored dianion species were similar, the four compounds showed large differences in color and maximum absorption and emission wavelengths. DFT calculations clarified that these differences were caused by repulsion between the oxygen anion at the 1 position and the oxygen atom of the pyran ring. These findings may help guide the development of new fluorescent dyes that emit in longer wavelength regions.

EXPERIMENTAL

Compound **8**.

A mixture of **11** (152.5 mg, 0.50 mmol) and 1,8-dihydroxynaphthalene (**12**, 79.2 mg, 0.50 mmol) in

toluene (3.0 mL) and methanesulfonic acid (1.5 mL) was stirred for 40 min at 60 ºC. The reaction mixture was poured into a mixture of EtOAc and water. The organic layer was separated, washed successively with water (twice) and brine, dried over Na_2SO_4 and evaporated under reduced pressure to give a residue. The residue was purified by column chromatography (SiO_2; *n*-hexane-EtOAc=5:1) to afford **8** (111.1 mg, 52%) as a brown powder.

8: brown powder; mp >259 ºC (decomp.); IR (KBr) 3446, 1763, 1635, 1522, 1448, 1362, 1286 cm^{-1}; ^{1}H-NMR (400 MHz, DMSO-*d*$_6$) δ 10.05 (s, 1H), 9.97 (s, 1H), 8.11 (dd, *J* = 7.2 Hz, 1.2 Hz, 1H), 7.84 (s, 1H), 7.82 – 7.74 (m, 2H), 7.73 (d, *J* = 9.2 Hz, 1H), 7.50 (d, *J* = 8.8 Hz, 1H), 7.47 (dd, *J* = 8.0 Hz, 8.0 Hz, 1H), 7.45 (s, 1H), 7.35 (d, *J* = 7.6 Hz, 2H), 7.22 (d, *J* = 2.0 Hz, 1H), 7.08 (d, *J* = 7.6 Hz, 1H), 6.99 (dd, *J* = 8.8 Hz, 2.0 Hz, 1H), 6.70 (d, *J* = 8.8 Hz, 1H); ^{13}C-NMR (100 MHz, DMSO-*d*$_6$) δ 168.9, 156.9, 154.9, 153.3, 148.3, 148.0, 136.8, 135.9, 135.9, 130.4, 130.0, 128.9, 127.8, 125.4, 125.1, 125.0, 124.1, 123.6, 118.8, 118.6, 116.5, 114.0, 112.4, 111.9, 111.0, 107.3, 82.8 (one peak overlapped); HRMS (ESI/FT-ICR-MS) Calcd for $C_{28}H_{16}O_5Na$ $(M + Na)^+$ 455.0890, found 455.0899.

Compound **14**.

A solution of *n*-BuLi (1.64 M *n*-hexane solution; 1.26 mL, 2.02 mmol) was added dropwise to a solution of **13** (250 mg, 1.01 mmol) in dry THF (6 mL) and dry HMPA (0.6 mL) under N_2 atmosphere at −78 ºC. After 40 min stirring, a solution of iodine (333 mg, 1.31 mmol) in THF (1.5 mL) was added dropwise to the solution. The resultant solution was stirred at −78 ºC for 2.3 h, and then allowed to warm to room temperature. The reaction mixture was poured into the mixed solvent of EtOAc and aqueous NH_4Cl solution. The organic layers were successively washed with aqueous sodium thiosulfate solution, water (twice) and brine, dried over Na_2SO_4, filtered, and concentrated under reduced pressure to dryness. The residue was purified by column chromatography (SiO_2; *n*-hexane-EtOAc, 3:1 → 1:1) to afford a mixture of **13** and compound A (366 mg, **13**: compound A was estimated 0.7:1 by ^{1}H NMR measurement). A solution of *n*-BuLi (1.64 M *n*-hexane solution; 0.45 mL, 0.74 mmol) was added dropwise to a solution of the above mixture (containing about 250 mg of compound **A**, 0.67 mmol) in dry THF (3 mL) under N_2 atmosphere at −78 ºC. After 10 min stirring, the solution of lithiated compound **A** in THF was added dropwise to a solution of phthalic anhydride (98.9 mg, 0.67 mmol) in dry THF (7 mL). The resultant solution was stirred at −78 ºC for 2 h, and then allowed to warm to room temperature. The reaction mixture was poured into the mixed solvent of EtOAc and aqueous NH_4Cl solution. The organic layers were successively washed with water (twice) and brine, dried over Na_2SO_4, filtered, and concentrated under reduced pressure to dryness. The residue was purified by column chromatography (SiO_2; *n*-hexane-EtOAc, 1:1) to afford **14** (96.1 mg, 20% for 2 steps) as pale yellow foam.

14: yellow foam; IR (KBr) 3444, 2929, 1718, 1666, 1624 cm^{-1}; ^{1}H-NMR (400 MHz, $CDCl_3$) δ 8.71 (s, 1H), 7.97 (d, *J* = 8.0 Hz, 1H), 7.59 – 7.47 (m, 2H), 7.41 – 7.30 (m, 4H), 6.97 (d, *J* = 7.6 Hz, 1H), 5.34 (s, 2H), 4.95 (s, 2H), 3.49 (s, 3H), 3.16 (s, 3H); ^{13}C-NMR (100 MHz, $CDCl_3$) δ 195.9, 171.3, 154.3, 153.7, 145.1, 137.9, 132.6, 130.4, 129.4, 129.3, 128.3, 127.7, 127.2, 120.8, 120.1, 110.0, 106.7, 94.6, 94.3, 56.4, 56.1 (one peak overlapped); HRMS (ESI/FT-ICR-MS) Calcd for $C_{22}H_{20}O_7Na$ $(M + Na)^+$ 419.1101, found 419.0923.

Compound **15.**

A solution of 4M hydrogen chloride in 1,4-dioxane (0.63 mL) was added dropwise to a solution of **14** (46.2 mg, 0.125 mmol) in 1,4-dioxane (2.5 mL) and stirred for 16 h at room temperature. The reaction mixture was poured into a mixture of EtOAc and water. The organic layer was separated, washed successively with water (twice) and brine, dried over Na_2SO_4 and evaporated to give a residue. The residue was purified by column chromatography (SiO_2; *n*-hexane/EtOAc=1/2) to furnish **15** (30.4 mg, 79%) as an yellow powder.

15: yellow powder; mp 95-97 ºC; IR (KBr) 3421, 2924, 1705, 1643, 1572 cm^{-1}; ^{1}H-NMR (400 MHz, CD_3OD) δ 8.17 (dd, *J* = 8.0 Hz, 0.8 Hz, 1H), 8.12 (s, 1H), 7.77 (ddd, *J* = 7.2 Hz, 7.2 Hz, 1.2 Hz, 1H), 7.70 (ddd, *J* = 7.2 Hz, 7.2 Hz, 1.2 Hz, 1H), 7.50 (dd, *J* = 7.4 Hz, 1.2 Hz, 1H), 7.30 (dd, *J* = 8.4 Hz, 7.2 Hz, 1H), 7.18 (s, 1H), 7.15 (d, *J* = 8.0 Hz, 1H), 6.56 (d, *J* = 7.6 Hz, 1H); ^{13}C-NMR (100 MHz, CD_3OD) δ 205.1, 168.7, 158.4, 156.2, 142.1, 140.8, 133.6, 132.0, 131.9, 131.6, 131.0, 130.9, 128.7, 122.2, 120.1, 118.0, 112.0, 106.7; HRMS (ESI/FT-ICR-MS) Calcd for $C_{18}H_{12}O_5Na$ $(M + Na)^+$ 331.0577, found 331.0589.

Compound **9**.

Compound **9** was synthesized from compound **15** and 1,6-dihydroxynaphthalene (**16**) in a similar manner to that for compound **8** with exception of purification; The residue was purified by column chromatography (SiO_2; *n*-hexane/EtOAc=4/1) to get a mixture of compounds **9** and **7**. The mixture was further purified by recycling HPLC (SiO_2, *n*-hexane/EtOAc=4/1 and 1% MeOH) to afford compound **9** and compound **7** in 11% and 7%, respectively.

9: red powder, mp >213 ºC (decomp.); IR (KBr) 3406, 2921, 2852, 1736, 1460, 1392 cm^{-1}; ^{1}H-NMR (400 MHz, DMSO-d_6) δ 10.33 (s, 1H), 10.20 (s, 1H), 8.48 (d, *J* = 9.2 Hz, 1H), 8.14 (dd, *J* = 6.8 Hz, 2.0 Hz, 1H), 8.05 (s, 1H), 7.84 – 7.77 (m, 2H), 7.66 (s, 1H), 7.46 – 7.36 (m, 4H), 7.31 (dd, *J* = 9.0 Hz, 2.8 Hz, 1H), 7.18 (d, *J* = 2.0 Hz, 1H), 6.78 (d, *J* = 7.2 Hz, 1H), 6.70 (d, *J* = 8.8 Hz, 1H); ^{13}C-NMR (100 MHz, DMSO-d_6) δ 169.0, 157.4, 153.3, 153.3, 148.1, 146.8, 136.2, 136.1, 135.4, 130.5, 129.0, 128.3, 125.3,

125.0, 124.2, 123.9, 123.6, 122.6, 122.2, 121.7, 119.2, 119.0, 117.5, 117.2, 112.5, 109.3, 107.0, 82.7; HRMS (ESI/FT-ICR-MS) Calcd for $C_{28}H_{16}O_5Na$ $(M + Na)^+$ 455.0890, found 455.0901.

Compound **10.**

Compound **10** was synthesized from compound **15** and 1,8-dihydroxynaphthalene (**12**) in 24% yield in a similar manner to that for compound **8**.

10; brown powder, mp >260 ºC (decomp.); IR (KBr) 3500, 1768, 1637, 1514, 1460, 1367 cm^{-1}; ^{1}H-NMR (400 MHz, DMSO-d_6) δ 10.31 (s, 1H), 10.02 (s, 1H), 8.14 (dd, *J* = 6.8 Hz, 1.2 Hz, 1H), 7.99 (s, 1H), 7.85 – 7.78 (m, 2H), 7.66 (s, 1H), 7.52 (d, *J* = 9.2 Hz, 1H), 7.48 (dd, *J* = 7.8 Hz, 2.0 Hz, 1H), 7.47 (d, *J* = 8.0 Hz, 1H), 7.40 – 7.35 (m, 3H), 7.09 (d, *J* = 8.0 Hz, 1H), 6.77 (d, *J* = 7.2 Hz, 1H), 6.74 (d, *J* = 8.4 Hz, 1H); ^{13}C-NMR (100 MHz, DMSO-d_6) δ 168.9, 154.9, 153.4, 153.2, 148.3, 147.9, 136.9, 136.1, 135.4, 131.7, 130.6, 128.9, 125.2, 125.1, 124.2, 123.8, 123.6, 122.2, 121.8, 118.8, 118.6, 117.6, 114.1, 112.8, 112.4, 111.7, 106.9, 82.7; HRMS (ESI/FT-ICR-MS) Calcd for $C_{28}H_{16}O_5Na$ $(M + Na)^+$ 455.0890, found 455.0904.

ACKNOWLEDGEMENTS

This study was supported in part by KAKENHI (Nos. 26293005 and 19H03355). This study was carried out using the Fourier transform ion cyclotron resonance mass spectrometer in the Joint Usage/Research Center at the Institute for Chemical Research, Kyoto University.

REFERENCES AND NOTES

1. For recent reviews, see; K. Kikuchi, *Chem. Soc. Rev.*, 2010, **39**, 2048; H. Kobayashi, M. Ogawa, R. Alford, P. L. Choyke, and Y. Urano, *Chem. Rev.*, 2010, **110**, 2620.
2. For recent modified fluoresceins and rhodamines, see; J. E. Whitaker, R. P. Haugland, and F. G. Prendergast, *Anal. Biochem.*, 1991, **194**, 330; M. W. Kryman, T. M. McCormick, and M. R. Detty, *Organometallics*, 2016, **35**, 1944; P. Hammershøj, E. Thyrhaug, P. Harris, P. K. Ek, T. L. Andresen, and M. H. Clausen, *Tetrahedron Lett.*, 2017, **58**, 1611; Q. Wang, K. Huang, S. Cai, C. Liu, X. Jiao, S. He, L. Zhaob, and X. Zeng, *Org. Biomol. Chem.*, 2018, **16**, 7163; L. G. Wang, I. Munhenzva, M. Sibrian-Vazquez, J. O. Escobedo, C. H. Kitts, F. R. Fronczek, and R. M. Strongin, *J. Org. Chem.*, 2019, **84**, 2585.
3. E. Azuma, N. Nakamura, K. Kuramochi, T. Sasamori, N. Tokitoh, I. Sagami, and K. Tsubaki, *J. Org. Chem.*, 2012, **77**, 3492; E. Azuma, K. Kuramochi, and K. Tsubaki, *Tetrahedron*, 2013, **69**, 1694.
4. M. Sibrian-Vazquez, J. O. Escobedo, M. Lowry, F. R. Fronczek, and R. M. Strongin, *J. Am. Chem. Soc.*, 2012, **134**, 10502.

5. L. G. Lee, G. M. Berry, and C.-H. Chen, *Cytometry*, 1989, **10**, 151; K. Xu, B. Tang, H. Huang, G. Yang, Z. Chen, P. Li, and L. An, *Chem. Commun*., 2005, 5974; W. M. F. Fabian, S. Schuppler, and O. S. Wolfbeis, *J. Chem. Soc., Perkin Trans. 2*, 1996, 853; K. Xu, X. Liu, and B. Tang, *ChemBioChem*, 2007, **8**, 453; Y. J. Yang, M. Lowry, X. Y. Xu, J. O. Escobedo, M. Sibrian-Vazquez, L. Wong, L. C. M. Schowalter, T. J. Jensen, F. R. Fronczek, I. M. Warner, and R. M. Strongin, *Proc. Natl. Acad. Sci. U.S.A.*, 2008, **105**, 8829.
6. Y. Yang, M. Lowry, C. M. Schowalter, S. O. Fakayode, J. O. Escobedo, X. Xu, H. Zhang, T. J. Jensen, F. R. Fronczek, I. M. Warner, and R. M. Strongin, *J. Am. Chem. Soc*., 2006, **128**, 14081.
7. J. F. Eastman and D. R. Larkin, *J. Am. Chem. Soc*., 1958, **80**, 2887.
8. Gaussian 09, Revision D.01, M. J. Frisch, G. W. Trucks, H. B. Schlegel, G. E. Scuseria, M. A. Robb, J. R. Cheeseman, G. Scalmani, V. Barone, B. Mennucci, G. A. Petersson, H. Nakatsuji, M. Caricato, X. Li, H. P. Hratchian, A. F. Izmaylov, J. Bloino, G. Zheng, J. L. Sonnenberg, M. Hada, M. Ehara, K. Toyota, R. Fukuda, J. Hasegawa, M. Ishida, T. Nakajima, Y. Honda, O. Kitao, H. Nakai, T. Vreven, J. A. Montgomery, Jr., J. E. Peralta, F. Ogliaro, M. Bearpark, J. J. Heyd, E. Brothers, K. N. Kudin, V. N. Staroverov, R. Kobayashi, J. Normand, K. Raghavachari, A. Rendell, J. C. Burant, S. S. Iyengar, J. Tomasi, M. Cossi, N. Rega, J. M. Millam, M. Klene, J. E. Knox, J. B. Cross, V. Bakken, C. Adamo, J. Jaramillo, R. Gomperts, R. E. Stratmann, O. Yazyev, A. J. Austin, R. Cammi, C. Pomelli, J. W. Ochterski, R. L. Martin, K. Morokuma, V. G. Zakrzewski, G. A. Voth, P. Salvador, J. J. Dannenberg, S. Dapprich, A. D. Daniels, Ö. Farkas, J. B. Foresman, J. V. Ortiz, J. Cioslowski, and D. J. Fox, Gaussian, Inc., Wallingford CT, 2009.